



1 **Long-term changes of nitrogen leaching and their contributions to lake**  
2 **eutrophication dynamics on the Yangtze Plain of China**

3 **Qi Guan<sup>a,b</sup>, Jing Tang<sup>c,d,\*</sup>, Lian Feng<sup>a</sup>, Stefan Olin<sup>c</sup>, Guy Schurgers<sup>b</sup>**

4 <sup>a</sup> School of Environmental Science and Engineering, Southern University of Science and Technology,  
5 Shenzhen 518055, Guangdong, China.

6 <sup>b</sup> Department of Geosciences and Natural Resource Management, University of Copenhagen,  
7 Copenhagen, Denmark.

8 <sup>c</sup> Department of Physical Geography and Ecosystem Science, Lund University, Lund, Sweden.

9 <sup>d</sup> Department of Biology, University of Copenhagen, Copenhagen, Denmark.

10 \* corresponding author: [jing.tang@nateko.lu.se](mailto:jing.tang@nateko.lu.se)

11 **Abstract**

12 Over the past half century, drastically increased chemical fertilizer have entered agricultural ecosystems  
13 to promote the crop production on the Yangtze Plain, potentially enhancing agricultural nutrient sources  
14 for eutrophication in freshwater ecosystems. However, long-term trends of nitrogen dynamics in  
15 terrestrial ecosystems and their impacts on eutrophication changes in this region remain poorly studied.  
16 Using a process-based ecosystem model, we investigated the temporal and spatial patterns of nitrogen  
17 use efficiency (NUE) and nitrogen leaching on the Yangtze Plain from 1979 to 2018. The agricultural  
18 NUE for the Yangtze Plain significantly decreased from 50 % in 1979 to 25% in 2018, with the largest  
19 decline of NUE in soybean, rice and rapeseed. Simultaneously, the leached nitrogen from cropland and  
20 natural land increased with annual rates of 4.5 kg N ha<sup>-1</sup> yr<sup>-2</sup> and 0.22 kg N ha<sup>-1</sup> yr<sup>-2</sup>, respectively, leading  
21 to an overall increase of nitrogen inputs to the fifty large lakes. We further examined the correlations  
22 between terrestrial nutrient sources (i.e., the leached nitrogen, total phosphorus sources, and industrial  
23 wastewater discharge) and the satellite-observed probability of eutrophication occurrence (PEO) at an  
24 annual scale, and showed that PEO was positively correlated with the changes in terrestrial nutrient  
25 sources for most lakes. Agricultural nitrogen and phosphorus sources were found to explain the PEO  
26 trends in lakes in the western and central part of Yangtze Plain, and industrial wastewater discharge



27 was associated with the PEO trends in eastern lakes. Our results revealed the importance of terrestrial  
28 nutrient sources for long-term changes in eutrophic status over the fifty lakes of the Yangtze Plain. This  
29 calls for sustainable nitrogen applications in agriculture systems to improve water quality of local lake  
30 ecosystems.

### 31 **1 Introduction**

32 For the past half century, China's demand for grain production has increased from 250 Mt in 1960 to  
33 648 Mt in 2010 along with the growing population, industrial development, and human-diet changes  
34 (Zhao et al., 2008; Wang and Davis, 1998). Substantial chemical fertilizers (i.e., 35 mega-tons, Mt,  
35 nitrogen fertilizers in 2014 (Yu et al., 2019) simultaneously entered agricultural ecosystems for the  
36 promotion of crop production. Although national grain production consequently increased from 132 Mt  
37 in 1950 to 607 Mt in 2014 (Yu et al., 2019), such a level of fertilization has enhanced nitrogen discharge  
38 to terrestrial and freshwater ecosystems, leading to a series of ecological and environmental concerns,  
39 such as soil nitrogen pollution, water quality deterioration, and phytoplankton blooms (Zhang et al.,  
40 2019; Wang et al., 2021; Qu and Fan, 2010). It was reported that approximately 14.5 Mt N yr<sup>-1</sup> was  
41 discharged to surface water ecosystems over the entire China for the period of 2010-2014, which largely  
42 exceeded the national safe level of nitrogen discharge (i.e., 5.2 Mt N yr<sup>-1</sup>) for the aquatic environment  
43 (Yu et al., 2019). Such human-related nutrient enrichment poses a big challenge for China's sustainable  
44 development goals (Wang et al., 2022).

45 The Yangtze Plain, with a human population of 340 million and agricultural area of 100 million hectares  
46 (Chen et al., 2020a; Hou et al., 2020), is experiencing unprecedented ecological and environmental  
47 issues (Guan et al., 2020; Feng et al., 2019). From 1990 to 2015, total crop production increased by 15 %  
48 at the expense of an increase of 89 % in nitrogen fertilizers over the Yangtze Plain (Xu et al., 2019).  
49 Consequently, more frequent nitrogen pollution was observed in soil and water. For example, heavy  
50 fertilizer usage and intensive livestock contributed to soil nitrogen pollution on the Yangtze River Delta  
51 for the past four decades, leading to soil deterioration and nitrogen discharge (Zhao et al., 2022).  
52 Nitrogen discharge related to human activities (i.e., fertilizer and manure applications, and human food  
53 waste) largely increased the nutrient loading and accelerated the degradation of water quality in the



54 Yangtze River since the 1990s (Chen et al., 2020b). Under the recent sustainable development plans  
55 proposed by national and local governments, managing nitrogen sources from urban and crop systems  
56 is envisaged to mitigate severe soil and water pollutions (Chen et al., 2020b; Zhao et al., 2022; Shi et  
57 al., 2020). However, for the Yangtze Plain with a variety of crops and crop managements, the lack of  
58 insights into long-term changes of nitrogen dynamics, such as fertilizer application, plant nitrogen  
59 uptake, and nitrogen leaching, has limited our solution of proposing effective policies in related to  
60 nutrient management.

61 According to the national surveys and satellite observations, the lakes on the Yangtze Plain experienced  
62 eutrophication and algal blooms for the past two decades (Guan et al., 2020; Brunier et al., 2014).  
63 Cyanobacteria blooms were reported to frequently occur in Taihu and Chaohu lakes, with the peak  
64 expanded extent reported for 2006 (Qin et al., 2019). Since then, the magnitudes of algal blooms  
65 significantly decreased from 2006 to 2013, and slightly increased again from 2013 to 2018 (Huang et  
66 al., 2020). Satellite observations revealed widespread and serious eutrophication issues in large lakes  
67 of the Yangtze Plain for the periods of 2003-2011 and 2017-2018, although significantly decreasing  
68 trends were found in 20 out of 50 lakes throughout the periods (Guan et al., 2020). Various laws and  
69 guidelines were implemented on regional and national scales to control eutrophication problems, such  
70 as the Guidelines on Strengthening Water Environmental Protection for Critical Lakes in 2008 and the  
71 Water Pollution Control Action Plan in 2015 (Huang et al., 2019). Nevertheless, the eutrophication  
72 issues are still challenging to control and improve under the scarcity of effective strategies for the whole  
73 Yangtze Plain.

74 To understand the primary causes of eutrophication in the lakes of the Yangtze Plain, previous studies  
75 have attempted to determine the contributions of riverine nutrient exports and lacustrine nutrient loading  
76 to algal blooms in individual lakes, such as Taihu and Chaohu lakes (Tong et al., 2017; Tong et al.,  
77 2021; Xu et al., 2015). Wang et al. (2019b) identified that diffuse sources contributed 90% to riverine  
78 exports of total dissolved nitrogen, and point sources discharged 52% of riverine phosphorus exports to  
79 Taihu Lake. Based on field-measured phytoplankton biomass and nutrient concentrations, algal blooms  
80 in Taihu Lake were primarily attributed to excessive nutrient loads from 1993 to 2015 (Zhang et al.,



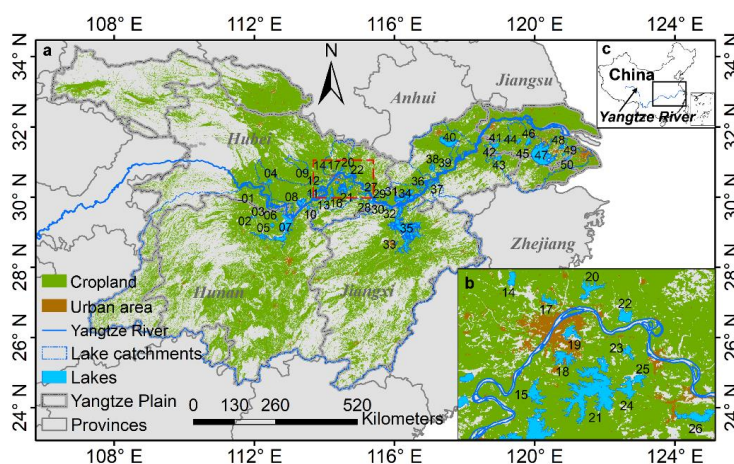
81 2018). Overloaded nutrients, in combination with climatic warming, were found to regulate the seasonal  
82 variations of cyanobacteria blooms in Chaohu Lake based on the monthly nutrient monitoring at discrete  
83 points (Tong et al., 2021). However, these studies only tracked the primary drivers of algal blooms for  
84 individual hyper-eutrophic lakes (i.e., Taihu and Chaohu lakes), which is insufficient to understand the  
85 causes of regional eutrophication and support the design of regional management strategies.  
86 Additionally, the studies above investigate cyanobacteria dynamics in relation to regional fertilizer use,  
87 but do not quantify changes in nitrogen uptake by vegetation.

88 In this study, we employed a process-based dynamic vegetation model, LPJ-GUESS (Smith et al., 2014),  
89 to investigate terrestrial nitrogen dynamics for the past four decades, examining the primary drivers of  
90 eutrophication trends in fifty large lakes of the Yangtze Plain (covering 63% of the whole plain). We  
91 simulated the vegetation dynamics, nitrogen cycles for agricultural and natural ecosystems from 1979  
92 to 2018, and then assessed the temporal trends of nitrogen use efficiency and nitrogen leaching. The  
93 terrestrial nutrient sources were used to examine their linkage with the satellite-derived eutrophication  
94 changes for fifty large lakes.

## 95 **2 Materials and Methods**

### 96 **2.1 Study area**

97 The Yangtze Plain (Fig. 1) is in the middle and lower basin of the Yangtze River. It covers a total area  
98 of  $7.8 \times 10^6$  km<sup>2</sup> from Hunan Province to Shanghai City, and accommodates approximately 5000  
99 freshwater lakes, ponds and reservoirs (Hou et al., 2017). Its sub-tropical monsoon climate provides  
100 annual mean temperature (~15°C) and precipitation (~1000 mm) conditions favorable for crop  
101 cultivations, in particular cereals and oil seeds, making the Yangtze Plain one of the top three food  
102 production regions in China. However, since the policy of Reform and Opening-up of China in the  
103 1980s (Zhang et al., 2010), agricultural ecosystems have been confronted with great pressure from  
104 urban expansion on the Yangtze Plain. Rapid urban expansion encroached on arable land, mainly on  
105 the eastern parts of the Yangtze Plain (Zhang et al., 2021).



106

107 **Figure 1.** Locations of the Yangtze Plain and the fifty large lakes studied here. (b) Detailed overview  
108 of Wuhan region (red box in (a)) and the surrounding lakes.

## 109 2.2 Dynamic vegetation model

110 We used a dynamic ecosystem model, LPJ-GUESS (Smith et al., 2014; Olin et al., 2015b), to simulate  
111 vegetation dynamics (i.e., the establishment, growth, competition, and mortality of plants), soil  
112 biogeochemistry, and carbon and nitrogen cycles for different ecosystems on the Yangtze Plain. The  
113 model has been widely used to assess ecosystem carbon and nitrogen fluxes at regional and global scales  
114 (Smith et al., 2014). Plant functional types (PFTs) and crop functional types (CFTs) are designed to  
115 describe the different types of plants and crops with a set of pre-defined bioclimatic and physiological  
116 parameters, such as photosynthetic pathways, phenology, growth forms and life history strategies for  
117 PFTs, as well as irrigation, fertilization, and rotation schemes for CFTs (Smith et al., 2014; Sitch et al.,  
118 2003; Olin et al., 2015a; Lindeskog et al., 2013).

119 Carbon and nitrogen fluxes between ecosystems and the atmosphere are calculated on a daily basis. For  
120 natural PFTs, net primary production (NPP) is accumulated and allocated to different plant  
121 compartments (i.e., leaves, roots, and sapwood and heartwood for trees) at the end of each simulation  
122 year. Soils are represented by 11 carbon and nitrogen pools with different decomposition rates (Parton  
123 et al., 1993; Parton et al., 2010), dependent on soil temperature and texture, water content, and base  
124 decay rates (Smith et al., 2014). Atmospheric deposition and plant biological fixation provide nitrogen



125 sources for plant growth and development, while the decomposition of soil organic matter can release  
126 mineral N into the soils and nitrogen-related gases into the atmosphere. Moreover, soil soluble nitrogen  
127 can also leach with the surface runoff in the forms of dissolved organic and inorganic nitrogen (i.e.,  
128 DON and DIN). In the model, leaching of DON is a function of the decay rates of soil microbial carbon  
129 pool and soil percolation, while DIN leaching depends on the available mineral nitrogen in soils and  
130 soil percolation, as well as soil water content.

131 Crop growth starts from a seedling with initial carbon and nitrogen masses at a prescribed sowing date.  
132 Chemical fertilizer and livestock manure supply external nitrogen for crop growth. Crop N uptake is  
133 simulated as the lesser between crop N demand and accessible mineral N in soils, where the former  
134 depends on crop development stages and C:N ratios of leaves and roots, and the latter is affected by soil  
135 temperature and fine root biomass (Olin et al., 2015a). Differing from natural PFTs, NPP is allocated  
136 to leaves and stems, root, and storage organs for each CFT on a daily basis, according to the daily  
137 allocation strategies related to crop development stages (Olin et al., 2015a).

### 138 **2.3 LPJ-GUESS input, calibration, and evaluation dataset**

#### 139 **2.3.1 Input data**

140 We ran LPJ-GUESS separating four land use types (natural land, cropland, pasture and urban) with a  
141 500-year spin-up to simulate the vegetation dynamics and the associated nitrogen fluxes for the Yangtze  
142 Plain from 1979 to 2018.

143 The gridded input data for LPJ-GUESS include climate, fractions of four land use types, total chemical  
144 fertilizer and manure application rates, cover fractions of each CFT within the cropland area, and soil  
145 properties. We used daily temperature, precipitation, and shortwave radiation provided by the China  
146 Meteorological Forcing Dataset (CMFD), with a spatial resolution of  $0.1^\circ$  and a temporal coverage of  
147 1979-2018 (He et al., 2020). The 300-m Climate Change Initiative Land Cover (CCI-LC version 2.0)  
148 dataset was regrouped into four different land use types (i.e., urban, cropland, pasture, and natural land)  
149 to obtain the cover fractions within each  $0.1^\circ$  grid cell for the period of 1992 to 2018 (Defourny et al.,  
150 2012) (see the details about regrouping process in Supplementary S1). Soil properties, i.e., fractions of



151 sand, clay and silt, organic carbon content, C:N, pH, and bulk density were extracted from the World  
152 Inventory of Soil Property Estimates (WISE30sec) dataset (Batjes, 2016). Based on the original data  
153 with a spatial resolution of 30 sec, we determined the dominant FAO soil type based on their relative  
154 area in each grid cell, and used its properties as input data for the grid cell. Gridded chemical fertilizer  
155 and manure application data were extracted from global fertilizer usage (Lu and Tian, 2017) and manure  
156 data (Zhang et al., 2017), which have spatial resolutions of 0.5° and 0.5°, respectively. We resampled  
157 the fertilizer and manure application data into the spatial resolution of 0.1° to represent the chemical  
158 fertilizer and manure application for each grid cell from 1979 to 2014.

159 The gridded fractions of CFTs were calculated based on observational data provided by the China  
160 Meteorological Data Service Center (<https://data.cma.cn/site/subjectDetail/id/101.html>). The dataset  
161 contains the information about the types, sowing and harvest dates for totally eleven crops at 92  
162 observational sites across the whole Yangtze Plain (listed in Table S1). An adaptive inverse distance  
163 weighting method was then used to interpolate the maps of the relative fractions of all crops, and their  
164 sowing and harvest dates for the period of 1992-2015 (see the details in Supplementary S2). Due to the  
165 limited availability for the period of 1979-1991 and 2016-2018, we used the same crop information (i.e.,  
166 the fractions of crop types, sowing and harvest dates) from the nearest years.

### 167 **2.3.2 Model calibration and evaluation data**

168 The model was calibrated based on the observed crop yield collected by the China Meteorological Data  
169 Service Center (<https://data.cma.cn/site/showSubject/id/102.html>). The dataset provides crop yield data  
170 for eight main crops collected at different numbers of sites (i.e., winter wheat (number of sites: 37),  
171 spring maize (6), summer maize (10), single-season rice (28), early-season rice (30), late-season rice  
172 (30), rapeseed (38), and soybean (15)), for the period of 2000-2013. For the Yangtze Plain, hybrid and  
173 super-hybrid rice are widely cultivated to obtain high grain yield within short growing seasons due to  
174 the enhanced photosynthetic rates associated with leaf-level chlorophyll and rubisco contents (Huang  
175 et al., 2016). However, the default parameters for rice CFTs in LPJ-GUESS cannot capture the high  
176 yield features of hybrid and super-hybrid rice. Therefore, we calibrated the relationship between the



177 leaf-based nitrogen content and the maximum catalytic capacity of rubisco (see the details in  
178 Supplementary S3). We randomly selected five sites with rice yield data from 2000 to 2013 as the  
179 calibration data, and the other rice yield data were used as the evaluation data. For parameters of other  
180 CFTs (listed in Table S1), the default values performed satisfactory in the comparison with all observed  
181 yield data (Fig. 2). It is noted that regional mean yield for each crop was derived from the evaluation  
182 data to compare the simulated values on the Yangtze Plain.

183 Simulated GPP and LAI were further compared with Global Solar-induced Chlorophyll Fluorescence  
184 Gross Primary Productivity (GOSIF GPP) and third generation of Global Inventory Modeling and  
185 Mapping Studies Leaf Area Index (GIMMS LAI3g) products to evaluate the performance of modelled  
186 vegetation variables. The global GOSIF GPP products have a spatial resolution of  $0.05^\circ$  and cover the  
187 period of 1992-2018 (Fang et al., 2019). Biweekly GIMMS LAI3g products with a spatial resolution of  
188  $0.25^\circ$  were obtained and then converted to annual mean LAI3g maps from 1982 to 2011 (Zhu et al.,  
189 2013).

190 The modelled responses of nitrogen leaching to different fertilizer applications were evaluated based  
191 on an observational dataset published in Gao et al. (2016), where they collected nitrogen leaching for  
192 plots with 3 or 4 different levels of nitrogen fertilizer inputs for maize, rice, and wheat. In our study, we  
193 selected the observed responses without influences of phosphorus and potash fertilizers on the Yangtze  
194 Plain as the evaluation data (two samples for each crop). For these sites, individual simulations were  
195 performed by assigning the full coverage of each corresponding crop grow, and prescribing the levels  
196 of nitrogen fertilizer applications as in the experimental site. It should be noted that we used the same  
197 nitrogen fertilizer applications in the period prior to the field experiment.

#### 198 **2.4 Assessment of long-term changes in nitrogen dynamics**

199 We assessed long-term changes of nitrogen use efficiency (NUE) and nitrogen leaching for the past  
200 four decades. A linear regression was conducted for the annual mean NUE and nitrogen leaching for  
201 the whole Yangtze Plain to determine the associated change rates (i.e., the regression slopes), and the  
202 significance was tested by a *t*-test. The mean leached nitrogen over the drainage area of all examined





203 lakes was calculated to explore long-term changes in terrestrial nitrogen sources for lake ecosystems,  
204 and the associated temporal trends were assessed by the linear regression and *t*-test.

## 205 **2.5 Examination of the primary driving forces of eutrophication dynamics**

### 206 **2.5.1 Satellite-derived eutrophication changes**

207 We used satellite-derived PEO data published in Guan et al. (2020) to represent the eutrophication  
208 changes for fifty large lakes on the Yangtze Plain. The PEO was defined as the frequency of high  
209 chlorophyll-*a* concentrations (i.e., > 10 mg m<sup>-3</sup>) or algal bloom occurrences in satellite imagery for each  
210 year. The averaged PEO values for pixels within each lake were then obtained to delineate the  
211 eutrophication status and changes in fifty large lakes of the Yangtze Plain during the MERIS (i.e., 2003-  
212 2011) and OLCI (i.e., 2017-2018) observational periods. However, due to un-availability of crop- and  
213 nitrogen-related data for the period of 2017-2018, we only used the PEO data derived from MERIS  
214 observations (i.e., 2003-2011) here to examine their primary driving forces.

### 215 **2.5.2 Examination of the correlations between nutrient and PEO anomalies**

216 To examine the impacts of terrestrial nutrient sources on eutrophication changes in fifty large lakes of  
217 the Yangtze Plain, we used the simulated nitrogen leaching (LN) and anthropogenic phosphorus sources  
218 (i.e., total phosphorus from chemical fertilizer and manure, TP) representing the agricultural nutrient  
219 sources, and industrial wastewater discharge (IW) representing industrial nutrient sources. The gridded  
220 phosphorus fertilizer data were extracted from a global dataset developed by Lu and Tian (2017), while  
221 the phosphorus content in manure was calculated based on the nitrogen contents of manure products  
222 and the associated N:P ratios of different animals' excrement (Table S3). Annual industrial wastewater  
223 discharge data were obtained from the China City Statistical Yearbook ([https://data.cnki.net/trade/Year-  
224 book/Single/N2018050234?zcode=Z011](https://data.cnki.net/trade/Year-book/Single/N2018050234?zcode=Z011)).

225 The 9-year's mean (2003-2011) of three nutrient-related variables (i.e., LN, TP and IW) were used in a  
226 principal component analysis (PCA) followed by a K-means clustering (Hartigan and Wong, 1979) to  
227 classify examined fifty lakes based on similarities of terrestrial nutrient sources. In this process, all  
228 variables were normalized (across all years and lakes) based on the z-score method to remove the

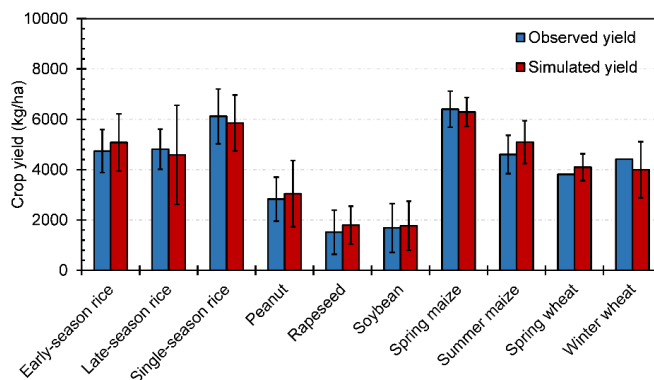


229 influence of different magnitudes in nutrient-related variables. We derived the first two principal  
230 components (PCs) from all normalized variables through a PCA, and the lakes were classified into three  
231 classes based on the first two PCs through the clustering methods. Finally, the annual anomalies of these  
232 nutrient-related variables and PEOs relative to their 9-year means were used to determine the primary  
233 drivers of temporal trends in eutrophication for each lake class.

### 234 3 Results

#### 235 3.1 Evaluation of LPJ-GUESS simulation

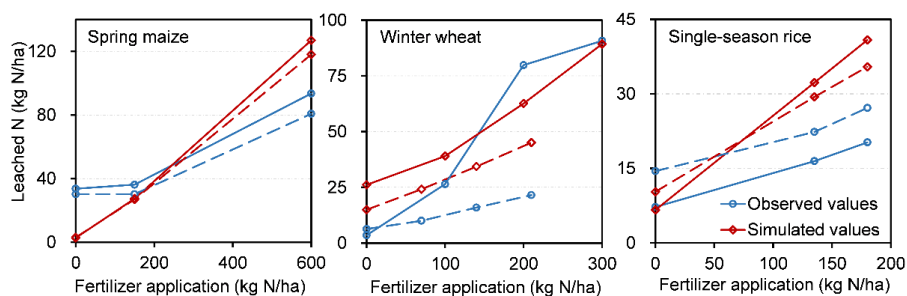
236 For the evaluation of LPJ-GUESS simulation for the past four decades, the simulated LAI, GPP and  
237 crop yield were compared with observation-based estimates. Mean crop yields agreed well with the  
238 observed values, with mean relative errors of  $< 10\%$  (Fig. 2). The comparison of simulated and observed  
239 LAI, and GPP were also satisfactory with overall high accuracy (i.e., a mean relative error of  $\sim 20\%$  and  
240 the root squared relative errors of  $< 30\%$ ) and spatial distributions consistent with observed patterns  
241 (Fig. S1 and S2). Considering the difference in spatial scales between the grid cells and the gridded  
242 evaluation data (i.e., the observed LAI and GPP maps), the overall performance of vegetation simulation  
243 over the different land use types were considered acceptable. In addition, the simulated responses of  
244 nitrogen leaching to different fertilizer applications at the experimental sites showed overall similar  
245 trends as the observation ones for all three crops (i.e., maize, rice, and wheat), despite varying  
246 magnitudes of differences between the simulated and observed leached nitrogen at certain fertilizer  
247 level (Fig. 3).



248



249 **Figure 2.** Comparison between the simulated and observed crop mean yields of different crops on the  
250 Yangtze Plain; the mean values were averaged over the period 2000-2015 and across totally 179 sites.  
251 Error bars show one standard deviation of crop yield.



252

253 **Figure 3.** The simulated and observed responses of the nitrogen leaching to different levels of fertilizer  
254 application rates for three main crop types (i.e., maize, rice, and wheat) over the Yangtze Plain.

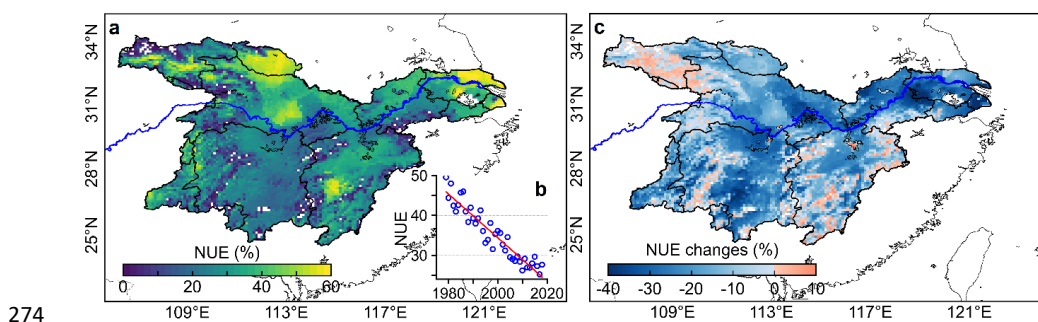
### 255 3.2 Long-term changes of nitrogen use efficiency over the Yangtze Plain

256 The climatological NUE was calculated to examine the spatial patterns of plant nitrogen uptake on the  
257 Yangtze Plain from 1979 to 2018. Considerable variations were detected across the entire Yangtze Plain,  
258 with NUE values ranging from 5% to 60% (Fig. 4a). Two hotspots of high NUE were in the Hubei and  
259 Jiangsu Province (see locations in Fig.1), dominated by cultivations of single-season rice and winter  
260 wheat under the moderate levels (i.e., ~200 kg N ha<sup>-1</sup> yr<sup>-1</sup>) of fertilizer applications (Fig. S3). The NUE  
261 values also differed among different crop types for the past four decades. The largest NUE values were  
262 found for soybean (74.0 % ± 11.0 %, Fig 5), while the lowest values were found for late-season rice  
263 (15.9% ± 4.3%).

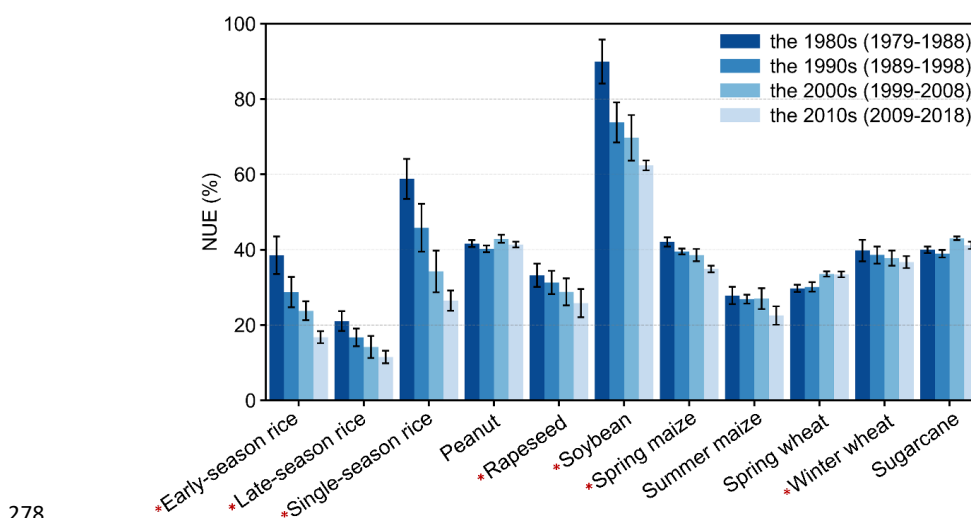
264 Due to the unprecedented increase of chemical fertilizer application since the 1980s, the crop NUE on  
265 the Yangtze Plain has significantly decreased from ca. 50% in 1979 to 25% in 2018 ( $p < 0.05$ , in Fig.  
266 4b), with an overall annual change rate of -0.55 % yr<sup>-1</sup>. Overall, regions with relatively high levels of  
267 NUE depicted a moderate or even slight increase for the past four decades, while the regions dominated  
268 low-level NUE (i.e., Hubei and Hunan provinces in Fig. 1) experienced strongly declining trends (Fig.



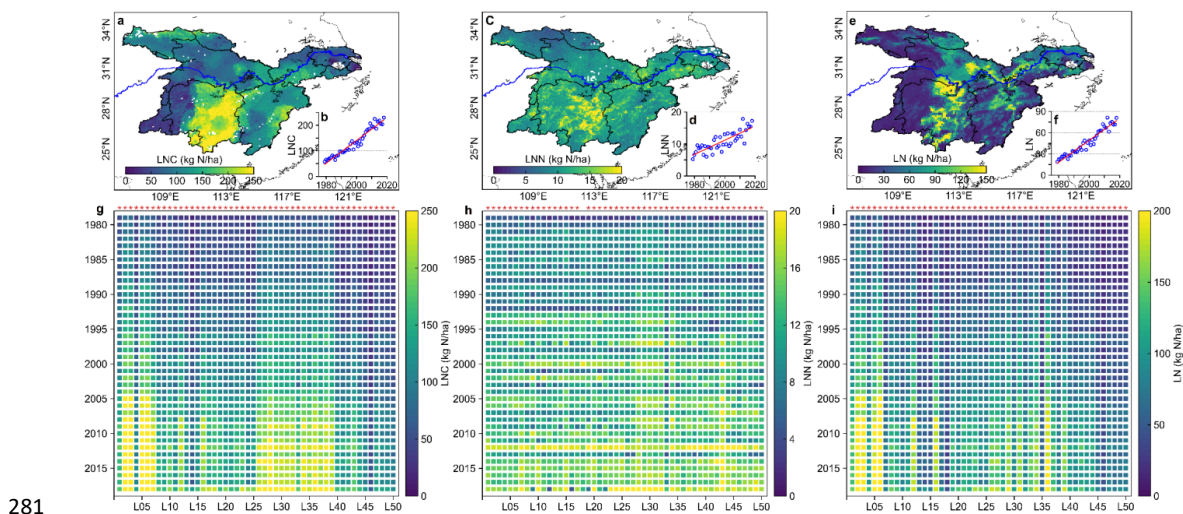
269 4a&4c), as a result of the enhanced fertilizer applications. Considerable differences in magnitudes and  
 270 trends of NUE were also examined among the crop types. Significant decreases (t-test,  $p < 0.05$ ) in the  
 271 decadal NUEs were found for seven crop types (annotated with “\*” in Fig. 5), with the largest decrease  
 272 for the double cropping of early- and late-season rice (Fig. 4c and S3). In contrast, three crop types  
 273 experienced increasing trends of NUE, including peanut, spring wheat, and sugarcane (Fig. 5).



274  
 275 **Figure 4.** Nitrogen use efficiency (NUE) on the Yangtze Plain from 1979 to 2018. (a) Spatial  
 276 distributions of climatological NUE (1979-2018), and the inset (b) shows the long-term trends of area  
 277 mean NUE; (c) Changes in NUE between the first (1979-1988) and the last (2009-2018) decades.



278  
 279 **Figure 5.** Decadal values of NUE for each crop functional type, averaged over the Yangtze Plain for  
 280 the past four decades. Significantly decreasing trends ( $p < 0.05$ ) are annotated with \* using a t-test.



281

282 **Figure 6.** Tempo-spatial patterns of leached nitrogen from cropland (LNC), natural land (LNN), and  
283 total leached nitrogen (LN) for the period of 1979-2018. Spatial distributions of climatological (a) LNC,  
284 (c) LNN, and (e) LN. The insets (b), (d) and (f) represent the long-term changes of mean LNC, LNN  
285 and LN, where the red lines are the linear fitting lines between years and nitrogen leaching. Inter-annual  
286 changes of (g) LNC, (h) LNN, and (i) LN for all examined lakes (L01-L50) from 1979 to 2018.  
287 Statistically significantly positive trends ( $p < 0.05$ ) are annotated with ‘\*’ on top of the panel, and see  
288 Fig. 1 for ID numbers of lakes.

### 289 3.3 Temporal and spatial patterns of nitrogen leaching for the past four decades

290 Along with the overall decreases in NUE, the leached nitrogen from agricultural (LNC, averaged across  
291 cropland area) and natural systems (LNN, averaged across natural area) experienced statistically  
292 significant increase ( $p < 0.05$ ) over the past four decades, with the different rates ( $4.5 \text{ kg N ha}^{-1}\text{yr}^{-2}$  and  
293  $0.22 \text{ kg N/ha /yr}^2$ , respectively in Fig. 6b, 6d). The LNC were an order of magnitude larger than the  
294 LNN. The high levels of LNC were found mainly in the Hunan Province (see Fig. 1 and Fig. 6a), with  
295 the average LNC value of  $149 \text{ kg N ha}^{-1} \text{ yr}^{-1}$ . In contrast, considerable spatial variations in LNN were  
296 revealed between the north and south parts of the Yangtze Plain (Fig. 6c).

297 To understand nitrogen sources for each corresponding lake ecosystems on the Yangtze Plain, we  
298 calculated the mean leached nitrogen (LN, averaged across ground area) over the drainage area of each



299 studied lake. The LN values ranged from 29 kg N ha<sup>-1</sup> yr<sup>-1</sup> in Gehu Lake (L46 in Fig. 6i) to 153 kg N  
300 ha<sup>-1</sup> yr<sup>-1</sup> in Donghu Lake (L05 in Fig. 6i), indicating the considerable difference between the western  
301 lakes in the Hunan Province and the eastern lakes in the Jiangsu Province. All examined lakes  
302 experienced statistically significantly increasing trends in the LN (t-test,  $p < 0.05$ ) over the past four  
303 decades (Fig. 6i), where the agricultural activities contributed 94 % ± 5 % to the LN changes.

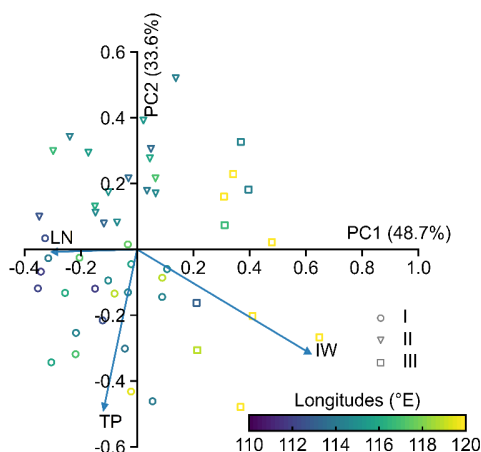
#### 304 **3.4 Driving forces of terrestrial nutrient sources to eutrophication changes**

305 The leached nitrogen, total phosphorus sources, and industrial wastewater discharge were used to  
306 represent terrestrial nutrient sources and were further investigated in terms of their linages to the  
307 observed PEOs. In the PCA analysis, the first two principal components (PCs) explained 48.7% and  
308 33.6% of variations in terrestrial nutrient sources (Fig. 7), where the first PC primarily depicts positive  
309 dependence on IW but negative links with LN, and the second PC reveals negative dependences on TP  
310 and IW. All fifty lakes were clustered into three classes based on the first two PCs (Fig. 7). Lakes in  
311 class I (n = 22) had the positive loading in the direction of the total phosphorus sources, with the main  
312 coverage of the middle Yangtze Plain (i.e., Jiangxi and Anhui Province in Fig. 1), while class II cover  
313 the most of lakes (n = 17) in the western regions (i.e., the Hunan Province and the western parts of the  
314 Hubei Province in Fig. 1). The lakes of class III (n = 11) are primarily located on the eastern Yangtze  
315 Plain, except for two lakes (i.e., Donghu and Tangxun lakes) which locate at the urban area of Wuhan  
316 City.

317 The correlations between annual anomalies of PEO and the three nutrient variables (relative to their  
318 means for 2003-2011) were examined for all three lake classes. The PEO anomalies were significantly  
319 correlated with different nutrient variables for three lake classes, indicating spatial variations of driving  
320 factors for eutrophication changes on the Yangtze Plain (Fig. 8). Specifically, both LN and TP  
321 anomalies exhibited significantly positive correlations ( $p < 0.001$ ) with the PEO trends in lakes of class  
322 I and II (Fig. 8a&b), indicating that the primary influence of agriculture-related sources to the increasing  
323 trends of PEO. In contrast, the annual PEO dynamics in lakes of class III showed a significantly positive  
324 correlation ( $p < 0.05$ ) with industrial wastewater discharge (Fig. 7c), meaning that the temporal trends  
325 of annual PEO in eastern parts of the Yangtze Plain were mainly associated with industrial wastewater

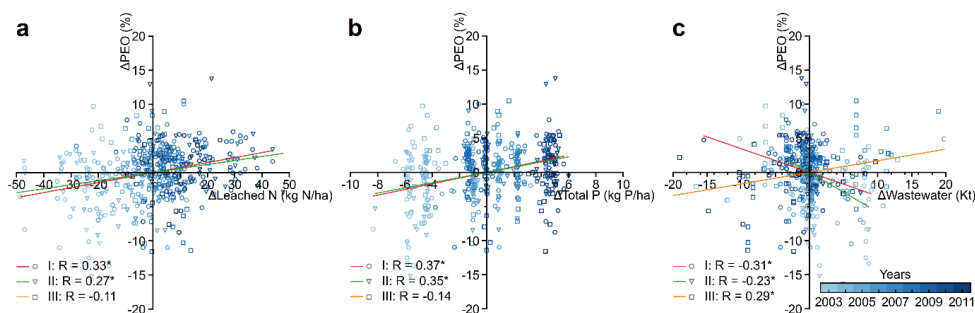


326 discharge. Note that the significantly negative correlations between the PEO and IW anomalies were  
 327 found for class I and II (Fig. 8c), which might be mechanistically unlikely. In such case, more efforts  
 328 are required in the future to determine the influence of industrial nutrient sources to eutrophication  
 329 changes in these lakes.



330

331 **Figure 7.** Loading plot of the principal component analysis (PCA) based on three nutrient-related  
 332 variables. The color of scattering points represent the distributions of lakes in longitudinal order, and  
 333 the directions of nutrient-related variables (i.e., LN leached nitrogen; TP total phosphorus sources; IW  
 334 industrial wastewater) were annotated with blue arrows.



335

336 **Figure 8.** Relationships between the annual anomalies of PEO and nitrogen leaching (a), total  
 337 phosphorus sources (b), and industrial wastewater discharge (c) for fifty studied lakes. The color and  
 338 symbol of scattering points represent the years and lake classes, and the colored lines (shown for



339 significant correlations only) are linear regression between the annual anomalies of PEO and nutrient-  
340 related variables for each lake classes.

#### 341 **4 Discussions**

##### 342 **4.1 Nitrogen use efficiency and driving forces of eutrophication changes.**

343 The overall low mean NUE (27 %) and declining trends in NUE ( $-0.55\% \text{ yr}^{-1}$ ) characterized agricultural  
344 ecosystems on the Yangtze Plain for the past four decades. Such decreasing trends are consistent with  
345 the previous studies using statistical datasets and numerical modelling (Zhang et al., 2015; Yu et al.,  
346 2019). However, the generally low NUE constitutes a vast gap with the targeted sustainable NUE of  
347 60% in China (Zhang et al., 2015), possibly leading to the excessive nitrogen discharge for terrestrial  
348 and aquatic ecosystems. The correlation analysis revealed that PEO trends in the western and central  
349 parts of the Yangtze Plain were associated with agricultural nutrient sources. As such, improving the  
350 NUE can decrease the agricultural nutrient exports to mitigate eutrophication issues in lake ecosystems,  
351 especially under the growing food demands in the future.

352 In the eastern parts of the Yangtze Plain, the correlation between industrial wastewater and PEO  
353 indicates that industrial sewage possibly delivered terrestrial nutrients to lakes from the adjacent cities,  
354 providing sufficient nutrient conditions for phytoplankton communities (Luan et al., 2007). The Jiangsu  
355 Province in the eastern parts of the Yangtze Plain (see the locations in Fig. 1) experienced rapid  
356 economic and industrial development since the policy of Reform and Opening-up of China since 1980s  
357 (Shen et al., 2020), which might be expected to result in enhanced industrial wastewater production,  
358 thereby triggering serious eutrophication in the lake systems. However, the national strategies and  
359 policies about green growth of industries encouraged reclamation of wastewater, investment on the  
360 advances in wastewater treatment technology and installment of municipal wastewater treatment plants  
361 (Li et al., 2013; Lyu et al., 2016). Industrial structures were also required to transform from secondary  
362 to tertiary industries under the environment-friendly targets of economic development (Huang et al.,  
363 2015). Consequently, industrial sewage showed decreasing trends and attributed to improvement of  
364 eutrophication status in the eastern Yangtze lakes.





365 **4.2 Limitations and Uncertainties**

366 Using the LPJ-GUESS model, we investigated the long-term changes and spatial variations of nitrogen  
367 dynamics (i.e., plant nitrogen uptake and nitrogen leaching) over the Yangtze Plain for the past four  
368 decades, and then examined the contributions of terrestrial nutrient sources to eutrophication changes  
369 in fifty large lakes. However, due to the lacking representation of a phosphorus cycle in the LPJ-GUESS  
370 model, we used external phosphorus fertilizer and manure application rates to represent the agricultural  
371 phosphorus sources, without consideration of potential impacts from plants and soil processes. Applied  
372 phosphorus is taken up through crop roots, or can be retained in soils (Schoumans, 2015) in variable  
373 degrees, affecting the export to lake ecosystems, which makes that the use of application data generates  
374 an uncertainty in our analysis. Nevertheless, we consider it important to consider the phosphorus  
375 sources as potential driving force for eutrophication changes under the low levels of phosphorus use  
376 efficiency over the Yangtze Plain (Li et al., 2017; Zheng et al., 2018).

377 Another source of uncertainty is associated with the potential impacts of terrestrial nutrient losses during  
378 the transport processes to surface water ecosystems, as well as the impacts of aquaculture-related  
379 nutrient sources. Transport processes depend on soil properties, topography, and hydrological  
380 conditions over the drainage area (Solomon et al., 2015; Tang et al., 2014; Tang et al., 2018), which is  
381 required to further consider at regional scales to estimate the dynamics of terrestrial nutrient exports for  
382 lake ecosystems on the Yangtze Plain. In addition, intensive and widespread freshwater aquaculture  
383 across the Yangtze Plain can contribute to accessible nutrient sources for the eutrophication  
384 development and phytoplankton growth (Guo and Li, 2003; Wang et al., 2019a). Satellite observations  
385 revealed that 17 out of 50 lakes on the Yangtze Plain have established enclosure fishery nets to increase  
386 the fish production (Dai et al., 2019). Consequently, substantial nutrients in fish food can directly enter  
387 aquaculture zones, promoting the contents of nitrogen and phosphorus in these lakes. These associated  
388 drivers are required to be comprehensively assessed to draw a complete picture of accessible nutrient  
389 sources for phytoplankton communities and then specify the anthropogenic impacts on water quality  
390 and eutrophication deterioration on the Yangtze Plain.



391 Uncertainties in the PEO data can originate from the uneven distributions of valid numbers of satellite  
392 observations across the fifty large lakes of the Yangtze Plain. Under the influence of observational  
393 conditions (i.e., cloud coverage and thick aerosols), the imagery with high-quality observations  
394 distributed unevenly across the different years and seasons, which potentially resulted in certain impacts  
395 on the derived annual PEOs and their temporal trends. Alternatively, the annual PEOs were calculated  
396 based on the quarterly values to minimize such uncertainties. Nevertheless, more frequent satellite  
397 observations will still be required to obtain a more accurate assessment of eutrophication changes in  
398 lake ecosystems.

## 399 **5 Conclusions**

400 We used the LPJ-GUESS model to investigate the long-term changes of nitrogen dynamics over the  
401 Yangtze Plain for the past four decades, and then examined their potential functions as the driving forces  
402 of eutrophication changes in fifty large lakes of the Yangtze Plain. Significant decreases in NUE  
403 dominated the whole Yangtze Plain, with the largest decrease in rice, soybean and rapeseed. The  
404 leached nitrogen from both cropland and natural land showed statistically significant increasing trends  
405 for all fifty examined lakes, indicating increased availability of terrestrial nitrogen sources in lake  
406 systems for the past four decades. Two classes of lakes located in the western and central parts of the  
407 Yangtze Plain showed significantly positive correlations between anomalies of PEO and agricultural  
408 nutrient sources (i.e., the leached nitrogen and total phosphorus sources), and the PEO anomalies in the  
409 remaining class (11 eastern lakes) were positively correlated with the industrial wastewater discharge.  
410 The impacts of agricultural and industrial nutrient sources to eutrophication changes further emphasize  
411 the importance of sustainable management of terrestrial nitrogen and phosphorus to improve water  
412 environments.

413 *Data availability.* Data used in this study are archived by the authors and are available upon request.

414 *Author contributions.* QG, JT, LF and GS designed the framework and methodology of the study. QG  
415 drafted a first version of the manuscript and analyzed the results. QG, JT and GS performed the



416 calibration of LPJ-GUESS model. All co-authors contributed critically to the manuscript editing and  
417 writing processes.

418 *Competing interests.* The authors declare that they have no conflict of interest.

419 *Acknowledgments.* This work was supported by the National Natural Science Foundation of China (NOs:  
420 41971304). Qi Guan was funded by the SUSTech-UCPH Joint Program. Jing Tang was financially  
421 supported by Swedish FORMAS mobility grant (2016-01580) and MERGE Short project. Stefan Olin  
422 acknowledges support from Lund University strong research areas MERGE and eSENCE. We are  
423 grateful to the European Space Agency (ESA) for publishing land cover dataset and to the China  
424 Meteorological Data Service Center for providing crop distribution and yield data.

#### 425 **References**

- 426 Batjes, N. H.: Harmonized soil property values for broad-scale modelling (WISE30sec) with estimates  
427 of global soil carbon stocks, *Geoderma*, 269, 61-68, 2016.
- 428 Brunier, G., Anthony, E. J., Goichot, M., Provansal, M., and Dussouillez, P.: Recent morphological  
429 changes in the Mekong and Bassac river channels, Mekong delta: The marked impact of river-bed  
430 mining and implications for delta destabilisation, *Geomorphology*, 224, 177-191, 2014.
- 431 Chen, X., Wang, L., Niu, Z., Zhang, M., and Li, J.: The effects of projected climate change and extreme  
432 climate on maize and rice in the Yangtze River Basin, China, *Agricultural and Forest Meteorology*, 282,  
433 107867, 2020a.
- 434 Chen, X., Strokhal, M., Kroeze, C., Supit, I., Wang, M., Ma, L., Chen, X., and Shi, X.: Modeling the  
435 contribution of crops to nitrogen pollution in the Yangtze River, *Environmental science & technology*,  
436 54, 11929-11939, 2020b.
- 437 Dai, Y., Feng, L., Hou, X., Choi, C.-Y., Liu, J., Cai, X., Shi, L., Zhang, Y., and Gibson, L.: Policy-driven  
438 changes in enclosure fisheries of large lakes in the Yangtze Plain: Evidence from satellite imagery,  
439 *Science of the total environment*, 688, 1286-1297, 2019.
- 440 Defourny, P., Kirches, G., Brockmann, C., Boettcher, M., Peters, M., Bontemps, S., Lamarche, C., Schlerf,  
441 M., and Santoro, M.: Land cover CCI, Product User Guide Version, 2, 325, 2012.
- 442 Fang, G., Yuan, T., Zhang, Y., Wen, X., and Lin, R.: Integrated study on soil erosion using RUSLE and GIS  
443 in Yangtze River Basin of Jiangsu Province (China), *Arabian Journal of Geosciences*, 12,  
444 10.1007/s12517-019-4331-2, 2019.
- 445 Feng, L., Hou, X., and Zheng, Y.: Monitoring and understanding the water transparency changes of fifty  
446 large lakes on the Yangtze Plain based on long-term MODIS observations, *Remote Sensing of  
447 Environment*, 221, 675-686, 2019.
- 448 Gao, S., Xu, P., Zhou, F., Yang, H., Zheng, C., Cao, W., Tao, S., Piao, S., Zhao, Y., and Ji, X.: Quantifying  
449 nitrogen leaching response to fertilizer additions in China's cropland, *Environmental pollution*, 211,  
450 241-251, 2016.
- 451 Guan, Q., Feng, L., Hou, X., Schurgers, G., Zheng, Y., and Tang, J.: Eutrophication changes in fifty large  
452 lakes on the Yangtze Plain of China derived from MERIS and OLCI observations, *Remote Sensing of  
453 Environment*, 246, 111890, 2020.
- 454 Guo, L. and Li, Z.: Effects of nitrogen and phosphorus from fish cage-culture on the communities of a  
455 shallow lake in middle Yangtze River basin of China, *Aquaculture*, 226, 201-212, 2003.
- 456 Hartigan, J. A. and Wong, M. A.: Algorithm AS 136: A k-means clustering algorithm, *Journal of the royal  
457 statistical society. series c*, 28, 100-108, 1979.



- 458 He, J., Yang, K., Tang, W., Lu, H., Qin, J., Chen, Y., and Li, X.: The first high-resolution meteorological  
459 forcing dataset for land process studies over China, *Scientific Data*, 7, 1-11, 2020.
- 460 Hou, X., Feng, L., Duan, H., Chen, X., Sun, D., and Shi, K.: Fifteen-year monitoring of the turbidity  
461 dynamics in large lakes and reservoirs in the middle and lower basin of the Yangtze River, China,  
462 *Remote Sensing of Environment*, 190, 107-121, 2017.
- 463 Hou, X., Feng, L., Tang, J., Song, X.-P., Liu, J., Zhang, Y., Wang, J., Xu, Y., Dai, Y., and Zheng, Y.:  
464 Anthropogenic transformation of Yangtze Plain freshwater lakes: Patterns, drivers and impacts,  
465 *Remote Sensing of Environment*, 248, 111998, 2020.
- 466 Huang, C., Zhang, M., Zou, J., Zhu, A.-x., Chen, X., Mi, Y., Wang, Y., Yang, H., and Li, Y.: Changes in land  
467 use, climate and the environment during a period of rapid economic development in Jiangsu Province,  
468 China, *Science of the Total Environment*, 536, 173-181, 2015.
- 469 Huang, J., Zhang, Y., Arhonditsis, G. B., Gao, J., Chen, Q., and Peng, J.: The magnitude and drivers of  
470 harmful algal blooms in China's lakes and reservoirs: A national-scale characterization, *Water Research*,  
471 181, 115902, 2020.
- 472 Huang, J., Zhang, Y., Arhonditsis, G. B., Gao, J., Chen, Q., Wu, N., Dong, F., and Shi, W.: How successful  
473 are the restoration efforts of China's lakes and reservoirs?, *Environment international*, 123, 96-103,  
474 2019.
- 475 Huang, M., Shan, S., Zhou, X., Chen, J., Cao, F., Jiang, L., and Zou, Y.: Leaf photosynthetic performance  
476 related to higher radiation use efficiency and grain yield in hybrid rice, *Field Crops Research*, 193, 87-  
477 93, 2016.
- 478 Li, A. A., Strokal, M. M., Bai, Z. Z., Kroeze, C. C., Ma, L. L., and Zhang, F. F.: Modelling reduced coastal  
479 eutrophication with increased crop yields in Chinese agriculture, *Soil Research*, 55, 506-517, 2017.
- 480 Li, Y., Luo, X., Huang, X., Wang, D., and Zhang, W.: Life cycle assessment of a municipal wastewater  
481 treatment plant: a case study in Suzhou, China, *Journal of cleaner production*, 57, 221-227, 2013.
- 482 Lindeskog, M., Arneth, A., Bondeau, A., Waha, K., Seaquist, J., Olin, S., and Smith, B.: Implications of  
483 accounting for land use in simulations of ecosystem carbon cycling in Africa, *Earth System Dynamics*,  
484 4, 385-407, 2013.
- 485 Lu, C. and Tian, H.: Global nitrogen and phosphorus fertilizer use for agriculture production in the past  
486 half century: shifted hot spots and nutrient imbalance, *Earth System Science Data*, 9, 181-192, 2017.
- 487 Luan, Q., Sun, J., Song, S., Shen, Z., and Yu, Z.: Canonical correspondence analysis of summer  
488 phytoplankton community and its environment in the Yangtze River estuary, China, *Chinese Journal of  
489 Plant Ecology*, 31, 445, 2007.
- 490 Lyu, S., Chen, W., Zhang, W., Fan, Y., and Jiao, W.: Wastewater reclamation and reuse in China:  
491 opportunities and challenges, *Journal of Environmental Sciences*, 39, 86-96, 2016.
- 492 Olin, S., Schurgers, G., Lindeskog, M., Wårlind, D., Smith, B., Bodin, P., Holmér, J., and Arneth, A.:  
493 Modelling the response of yields and tissue C: N to changes in atmospheric CO<sub>2</sub> and N management  
494 in the main wheat regions of western Europe, *Biogeosciences*, 12, 2489-2515, 2015a.
- 495 Olin, S., Lindeskog, M., Pugh, T., Schurgers, G., Wårlind, D., Mishurov, M., Zaehle, S., Stocker, B. D.,  
496 Smith, B., and Arneth, A.: Soil carbon management in large-scale Earth system modelling: implications  
497 for crop yields and nitrogen leaching, *Earth System Dynamics*, 6, 745-768, 2015b.
- 498 Parton, W., Scurlock, J., Ojima, D., Gilmanov, T., Scholes, R., Schimel, D. S., Kirchner, T., Menaut, J. C.,  
499 Seastedt, T., and Garcia Moya, E.: Observations and modeling of biomass and soil organic matter  
500 dynamics for the grassland biome worldwide, *Global biogeochemical cycles*, 7, 785-809, 1993.
- 501 Parton, W. J., Hanson, P. J., Swanston, C., Torn, M., Trumbore, S. E., Riley, W., and Kelly, R.: ForCent  
502 model development and testing using the Enriched Background Isotope Study experiment, *Journal of  
503 Geophysical Research: Biogeosciences*, 115, 2010.
- 504 Qin, B., Paerl, H. W., Brookes, J. D., Liu, J., Jeppesen, E., Zhu, G., Zhang, Y., Xu, H., Shi, K., and Deng, J.:  
505 Why Lake Taihu continues to be plagued with cyanobacterial blooms through 10 years (2007–2017)  
506 efforts, *Science Bulletin*, 64, 2019.
- 507 Qu, J. and Fan, M.: The current state of water quality and technology development for water pollution  
508 control in China, *Critical reviews in environmental science & technology*, 40, 519-560, 2010.



- 509 Schoumans, O. F.: Phosphorus leaching from soils: process description, risk assessment and mitigation,  
510 Wageningen University and Research 2015.
- 511 Shen, F., Yang, L., He, X., Zhou, C., and Adams, J. M.: Understanding the spatial–temporal variation of  
512 human footprint in Jiangsu Province, China, its anthropogenic and natural drivers and potential  
513 implications, *Scientific reports*, 10, 1-12, 2020.
- 514 Shi, X., Hu, K., Batchelor, W. D., Liang, H., Wu, Y., Wang, Q., Fu, J., Cui, X., and Zhou, F.: Exploring  
515 optimal nitrogen management strategies to mitigate nitrogen losses from paddy soil in the middle  
516 reaches of the Yangtze River, *Agricultural Water Management*, 228, 105877, 2020.
- 517 Sitch, S., Smith, B., Prentice, I. C., Arneth, A., Bondeau, A., Cramer, W., Kaplan, J. O., Levis, S., Lucht,  
518 W., and Sykes, M. T.: Evaluation of ecosystem dynamics, plant geography and terrestrial carbon cycling  
519 in the LPJ dynamic global vegetation model, *Global change biology*, 9, 161-185, 2003.
- 520 Smith, B., Wårlind, D., Arneth, A., Hickler, T., Leadley, P., Siltberg, J., and Zaehle, S.: Implications of  
521 incorporating N cycling and N limitations on primary production in an individual-based dynamic  
522 vegetation model, *Biogeosciences*, 11, 2027-2054, 2014.
- 523 Solomon, C. T., Jones, S. E., Weidel, B. C., Buffam, I., Fork, M. L., Karlsson, J., Larsen, S., Lennon, J. T.,  
524 Read, J. S., and Sadro, S.: Ecosystem consequences of changing inputs of terrestrial dissolved organic  
525 matter to lakes: current knowledge and future challenges, *Ecosystems*, 18, 376-389, 2015.
- 526 Tang, J., Pilesjö, P., Miller, P. A., Persson, A., Yang, Z., Hanna, E., and Callaghan, T. V.: Incorporating  
527 topographic indices into dynamic ecosystem modelling using LPJ - GUESS, *Ecohydrology*, 7, 1147-1162,  
528 2014.
- 529 Tang, J., Yurova, A. Y., Schurgers, G., Miller, P. A., Olin, S., Smith, B., Siewert, M. B., Olefeldt, D., Pilesjö,  
530 P., and Poska, A.: Drivers of dissolved organic carbon export in a subarctic catchment: Importance of  
531 microbial decomposition, sorption-desorption, peatland and lateral flow, *Science of the Total  
532 Environment*, 622, 260-274, 2018.
- 533 Tong, Y., Xiwen, X., Miao, Q., Jingjing, S., Yiyan, Z., Wei, Z., Mengzhu, W., Xuejun, W., and Yang, Z.:  
534 Lake warming intensifies the seasonal pattern of internal nutrient cycling in the eutrophic lake and  
535 potential impacts on algal blooms, *Water Research*, 188, 116570, 2021.
- 536 Tong, Y., Zhang, W., Wang, X., Couture, R.-M., Larssen, T., Zhao, Y., Li, J., Liang, H., Liu, X., and Bu, X.:  
537 Decline in Chinese lake phosphorus concentration accompanied by shift in sources since 2006, *Nature  
538 Geoscience*, 10, 507-511, 2017.
- 539 Wang, D., Zhang, S., Zhang, H., and Lin, S.: Omics study of harmful algal blooms in China: Current status,  
540 challenges, and future perspectives, *Harmful algae*, 107, 102079, 2021.
- 541 Wang, J., Beusen, A. H., Liu, X., and Bouwman, A. F.: Aquaculture production is a large, spatially  
542 concentrated source of nutrients in Chinese freshwater and coastal seas, *Environmental science &  
543 technology*, 54, 1464-1474, 2019a.
- 544 Wang, L. and Davis, J.: Can China Feed its People into the Next Millennium? Projections for China's  
545 grain supply and demand to 2010, *International Review of Applied Economics*, 12, 53-67, 1998.
- 546 Wang, M., Janssen, A. B., Bazin, J., Stokal, M., Ma, L., and Kroeze, C.: Accounting for interactions  
547 between Sustainable Development Goals is essential for water pollution control in China, *Nature  
548 communications*, 13, 1-13, 2022.
- 549 Wang, M., Stokal, M., Burek, P., Kroeze, C., Ma, L., and Janssen, A. B.: Excess nutrient loads to Lake  
550 Taihu: Opportunities for nutrient reduction, *Science of the Total Environment*, 664, 865-873, 2019b.
- 551 Xu, H., Paerl, H., Qin, B., Zhu, G., Hall, N., and Wu, Y.: Determining critical nutrient thresholds needed  
552 to control harmful cyanobacterial blooms in eutrophic Lake Taihu, China, *Environmental science &  
553 technology*, 49, 1051-1059, 2015.
- 554 Xu, X., Hu, H., Tan, Y., Yang, G., Zhu, P., and Jiang, B.: Quantifying the impacts of climate variability and  
555 human interventions on crop production and food security in the Yangtze River Basin, China, 1990–  
556 2015, *Science of the Total Environment*, 665, 379-389, 2019.
- 557 Yu, C., Huang, X., Chen, H., Godfray, H. C. J., Wright, J. S., Hall, J. W., Gong, P., Ni, S., Qiao, S., and  
558 Huang, G.: Managing nitrogen to restore water quality in China, *Nature*, 567, 516-520, 2019.



- 559 Zhang, B., Tian, H., Lu, C., Dangal, S. R., Yang, J., and Pan, S.: Global manure nitrogen production and  
560 application in cropland during 1860–2014: a 5 arcmin gridded global dataset for Earth system  
561 modeling, *Earth System Science Data*, 9, 667-678, 2017.
- 562 Zhang, C., Ju, X., Powlson, D., Oenema, O., and Smith, P.: Nitrogen surplus benchmarks for controlling  
563 N pollution in the main cropping systems of China, *Environmental science & technology*, 53, 6678-  
564 6687, 2019.
- 565 Zhang, M., Shi, X., Yang, Z., Yu, Y., Shi, L., and Qin, B.: Long-term dynamics and drivers of phytoplankton  
566 biomass in eutrophic Lake Taihu, *Science of the Total Environment*, 645, 876-886, 2018.
- 567 Zhang, N., Gao, Z., Wang, X., and Chen, Y.: Modeling the impact of urbanization on the local and  
568 regional climate in Yangtze River Delta, China, *Theoretical and applied climatology*, 102, 331-342, 2010.
- 569 Zhang, X., Davidson, E. A., Mauzerall, D. L., Searchinger, T. D., Dumas, P., and Shen, Y.: Managing  
570 nitrogen for sustainable development, *Nature*, 528, 51-59, 2015.
- 571 Zhang, Y., Sun, M., Yang, R., Li, X., Zhang, L., and Li, M.: Decoupling water environment pressures from  
572 economic growth in the Yangtze River Economic Belt, China, *Ecological Indicators*, 122, 107314, 2021.
- 573 Zhao, J., Luo, Q., Deng, H., and Yan, Y.: Opportunities and challenges of sustainable agricultural  
574 development in China, *Philosophical Transactions of the Royal Society B: Biological Sciences*, 363, 893-  
575 904, 2008.
- 576 Zhao, S., Chen, Y., Gu, X., Zheng, M., Fan, Z., Luo, D., Luo, K., and Liu, B.: Spatiotemporal variation  
577 characteristics of livestock manure nutrient in the soil environment of the Yangtze River Delta from  
578 1980 to 2018, *Scientific Reports*, 12, 1-17, 2022.
- 579 Zheng, J., Wang, W., Cao, X., Feng, X., Xing, W., Ding, Y., Dong, Q., and Shao, Q.: Responses of  
580 phosphorus use efficiency to human interference and climate change in the middle and lower reaches  
581 of the Yangtze River: historical simulation and future projections, *Journal of Cleaner Production*, 201,  
582 403-415, 2018.
- 583 Zhu, Z., Bi, J., Pan, Y., Ganguly, S., Anav, A., Xu, L., Samanta, A., Piao, S., Nemani, R. R., and Myneni, R.  
584 B.: Global data sets of vegetation leaf area index (LAI) 3g and fraction of photosynthetically active  
585 radiation (FPAR) 3g derived from global inventory modeling and mapping studies (GIMMS) normalized  
586 difference vegetation index (NDVI3g) for the period 1981 to 2011, *Remote sensing*, 5, 927-948, 2013.

587